Modelling and propagation of optical wave fields with scalar diffraction theory

Faye D. Espalmado*

National Institute of Physics, University of the Philippines Diliman
*Corresponding author: fdespalmado99@gmail.com

Abstract

Here we explore the formation of optical fields through the method of scalar diffraction theory. Simulations of the evolution of the propagating wave fieldwere conducted using MATLAB with the implementation of the Rayleigh Sommerfeld convolution approach. Varying the input amplitude, phase, and distance of the optical planes were also considered in the modelling process.

Keywords: formation of optical fields, scalar diffraction theory

1 Introduction

The electric and magnetic field of light is linked by the Maxwell's equations, under the assumption that the field can be approximated by a complex scalar potential and operates in a paraxial scale. In a homogeneous and isotropic medium, such as free space, the Maxwell's equations can be used to derive the Hemholtz equation. The scalar function given by:

$$U(P,t) = Re[U(P)exp(-i2\pi vt)]$$

$u(\mathbf{r})$ must satisfy the Hemholtz equation. This serves as the foundation of the scalar wave theory. Solutions to the wave diffraction problem has long been obtained, particularly the Fresnel-Kirchhoff (FK) and Rayleigh Sommerfeld (RS) diffraction formulas[1]. The RS Diffraction formula is given by:

$$U_I(P_0) = -\frac{1}{2\pi}\iint\limits_{\Sigma} U\frac{\partial G_K}{\partial n}ds \tag{1}$$

$$U_{II}(P_0) = \frac{1}{2\pi}\iint\limits_{\Sigma} \frac{\partial U}{\partial n}G_K ds \tag{2}$$

The scalar theory of diffraction is a significant concept considered in the study of the propagation of electromagnetic waves. This paper explores how to model an optical field following the scalar diffraction theory. Wave propagation was demonstrated via computer simulation based on the RS diffraction and transfer function. The effect of different parameters such as the input amplitude, input phase and distance between the input and output planes was also investigated.

2 Convolution approach to wave propagation

Numerical technique used in this paper to calculate the Fresnel diffraction patterns was the RS convolution method. The paraxial diffraction formula is essentially a convolution relation, thus the method of convolution was utilized to simulate the wave propagation of several set-ups. The process convolution is performed in the Fourier domain[2].

The angular spectrum determines the wave field amplitude through the Fourier expansion:

$$U(x,y) = F^{-1}\{G_{RS}(x,y,d)\cdot F[U(x',y')]\} \tag{3}$$

The convolution is calculated by multiplying the Fourier transform of the input field by the RS transfer function given by:

$$G_{RS} = exp[(i2\pi z/\lambda)\sqrt{1-(\lambda f_x)^2-(\lambda f_y)^2}] \tag{4}$$

where d corresponds to the distance, λ is the wavelength of the propagated optical field, and f_x and f_y are the spatial frequencies along the x and y axes, respectively[3].In this paper, λ is set at 0.5mm.

The simulations were performed in MATLAB where the algorithm described above was implemented.

3 Varying of input parameters

3.1 Input amplitudes

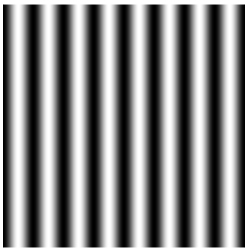
(a) Sinusoidal

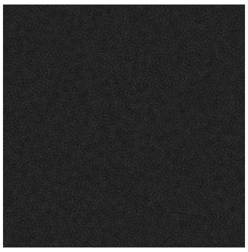
(b) Random

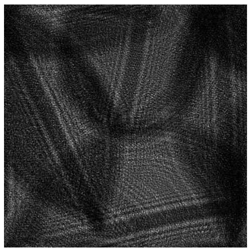
(c) Leaves

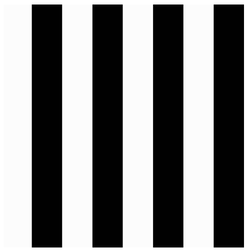
(d) Sinusoidal

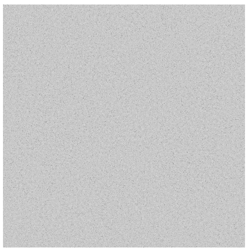
(e) Random

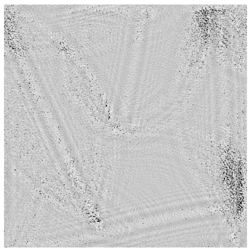
(f) Leaves

Figure 1: Amplitude ((a)-(c) and the corresponding phase distributions ((d)-(f)) in the output plane for different input amplitudes.

Varied input amplitudes were simulated with constant input phase distributions. A sinusoidal image was used in Figure 1(a),(d). The output amplitude resulted in a sinusoidal image also, with deeper or darker crests compared to the input amplitude distribution. The resulting phase distribution is a grating. A matrix of random values was used for Figures 1(b),(e). The output distributions are similar to the noise on the input amplitudes but the grey levels are varied across the distributions. For the leaves image in Figures 1(c),(f), the diffraction occurs around the veins and the outline of the leaves.

3.2 Input phase

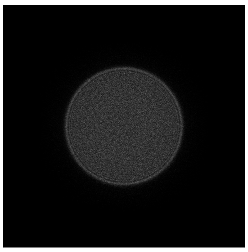
(a) Random

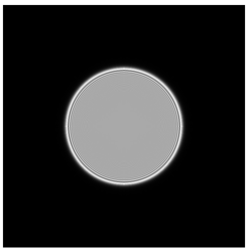
(b) Spherical

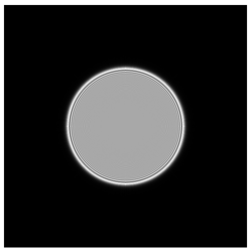
(c) Linear

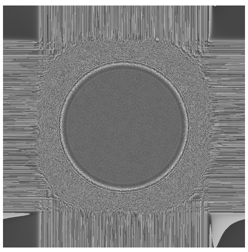
(d) Random

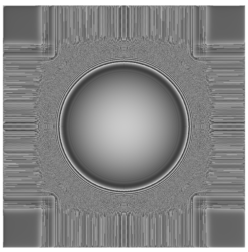
(e) Spherical

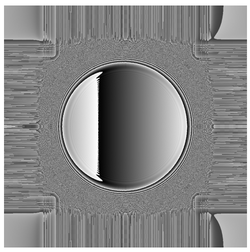
(f) Linear

Figure 2: Amplitude ((a)-(c) and the corresponding phase distributions ((d)-(f)) in the output plane with different input phase distributions.

Wave propagation for a circular aperture was simulated with random, spherical with focal length of 250, and linear input phase distributions.

Output amplitude distribution with the randomly-generated phase resulted in a random distribution with the circular mask. For spherical and linear phase distributions, the output amplitudes have the almost identical patterns within the circle.

The output phase distribution shows more variation among the input parameters. The distribution with the circular area adapted the distribution given by the phase of the input field.

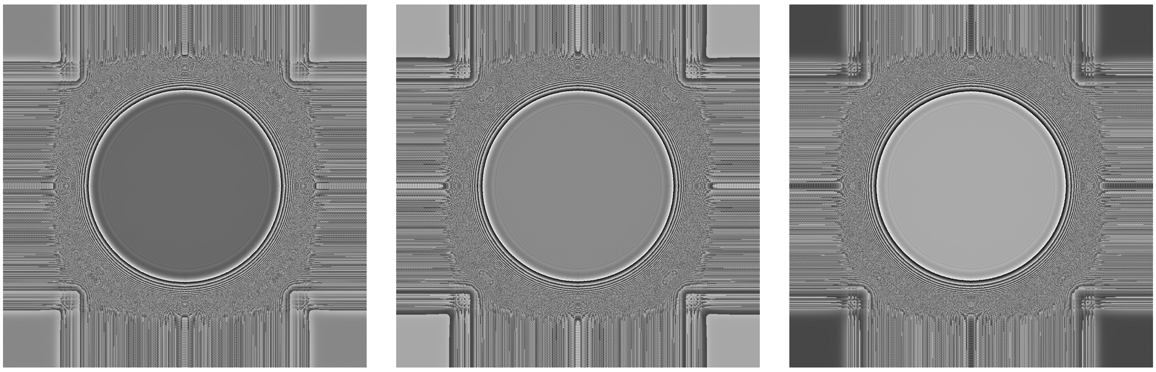

(a) $\pi/4$ (b) $\pi/2$ (c) $3\pi/4$

Figure 3: Output phase distribution with varying phase depth

The propagation for a circular aperture with constant phase distribution and varying phase depth was also examined. As shown in Figure 3, the gray level becomes lighter as the phase depth approaches π.

3.3 Varying distance between object and observation planes

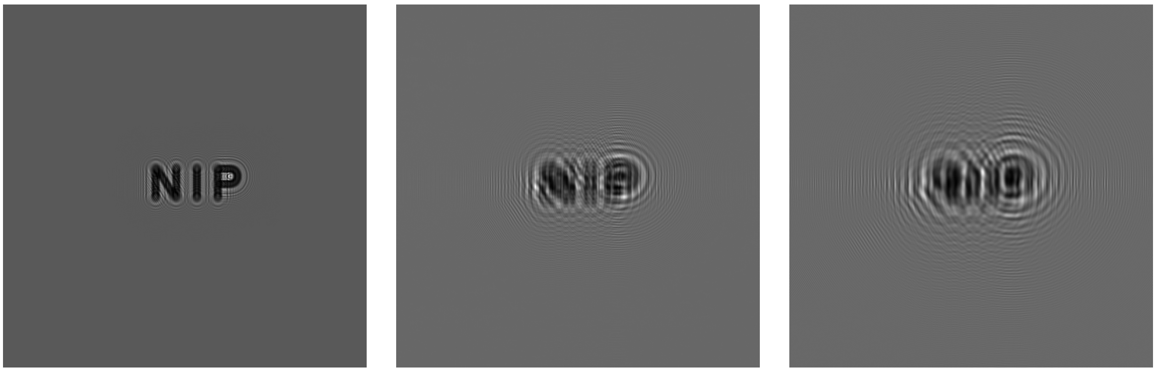

(a) 0.01mm (b) 0.05mm (c) 0.1mm

(d) 0.01mm (e) 0.05mm (f) 0.1mm

Figure 4: Amplitude ((a)-(c) and the corresponding phase distributions ((d)-(f)) in the output plane with varying distances between the object and observation planes

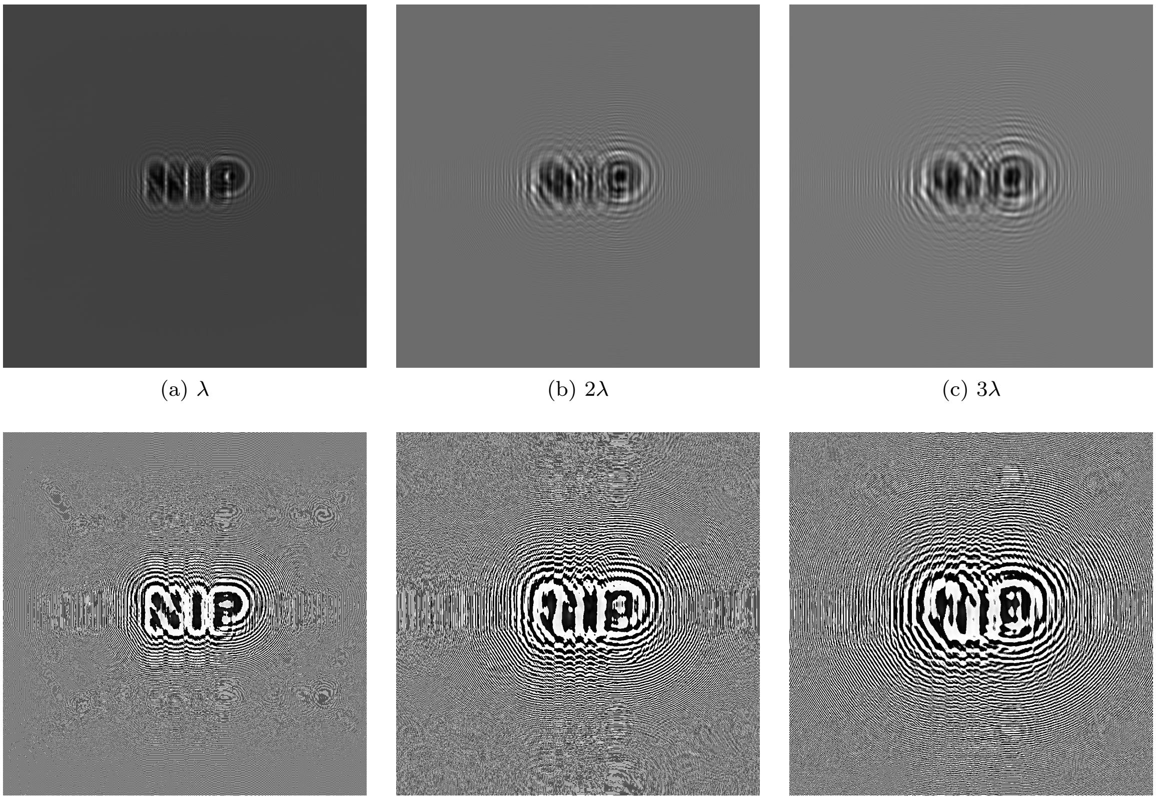

(a) λ (b) 2λ (c) 3λ

(d) λ (e) 2λ (f) 3λ

Figure 5: Amplitude ((a)-(c) and the corresponding phase distributions ((d)-(f)) in the output plane with varying distances in integer multiples of λ between the object and observation planes

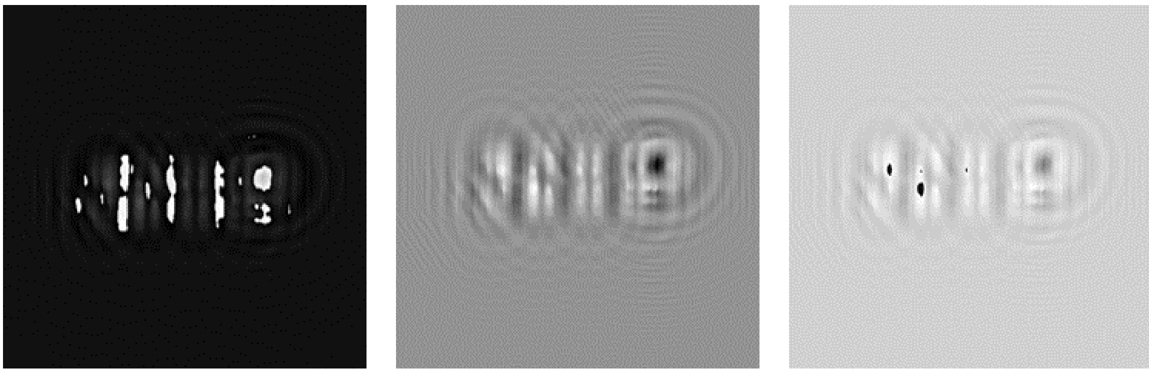

(a) $\lambda/8$ (b) $\lambda/2$ (c) $7\lambda/8$

Figure 6: Amplitude ((a)-(c) and the corresponding phase distributions ((d)-(f)) in the output plane with varying distances in fractions of λ between the object and observation planes

The distance d between the object and observation planes were varied for an input field composed of an aperture of "NIP" letters. The distances were varied in millimeters, integer multiples of λ, and fraction of λ.

As shown in Figure 4, the output phase and amplitude diffracts until the letters are almost ineligible as the distance increases. Gray levels vary for the output distributions.

The same trend is also apparent for multiples of λ, given in Figure 5. However, the output phase distribution shows more evident diffraction around the background of the field, wherein the gray levels are constant in all variations.

For fractions of λ, the output amplitude is the same for all variations. Figure 6 shows that the general pattern is for the output phase are similar throughout. However, the gray level varies such that it gets lighter as it approaches λ.

3.3.1 Propagation along xz plane

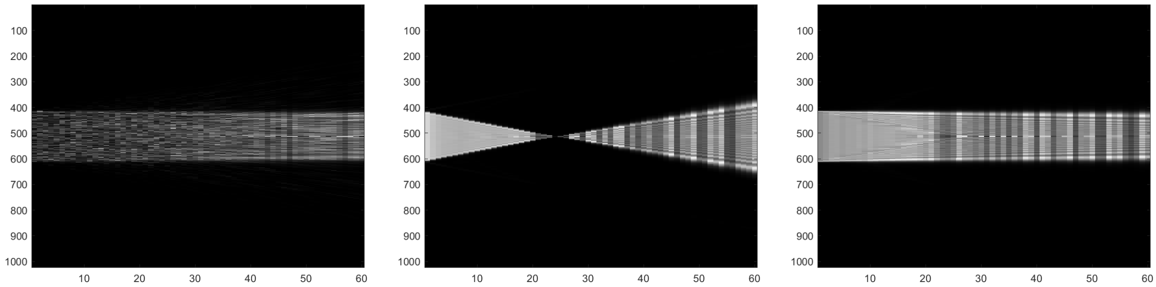

(a) Random (b) Spherical (c) Linear

Figure 7: Wave propagation along xz axis for varying phase distribution

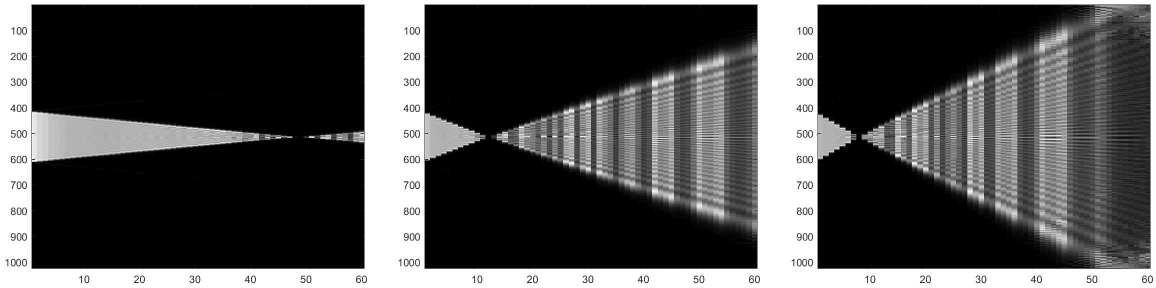

(a) $\lambda/2$ (b) 2λ (c) 3λ

Figure 8: Wave propagation along xz axis for varying wavelengths

The wave propagation of a circular disk along the xz plane was also observed. In Figure 7, random, linear and spherical phase distributions were tested. The spherical phase distribution has a focal length of 15.

Figure 8 describes the wave propagation along the xz plane for a circular disk with a spherical phase distribution of focal length 15.

4 Conclusions

In this paper, the method of using scalar diffraction theory to obtain optical wave fronts with different parameters was studied. Numerical calculation of the propagating wave field was performed using the RS convolution approach.

References

[1] J. Goodman, *Introduction to Fourier Optics* (Roberts and Company Publishers; 3rd edition, 2004).

[2] J. L. C. J. R. Sheppard and S. S. Kou, Rayleigh–sommerfeld diffraction formula in k space, *J. Opt. Soc. Am. A* **30**, 1180 (2013).

[3] T. Vovk and N. Petrov, Investigation of the methods for optical wavefront parameter manipulation, *J. Phys.: Conf. Ser.* **929**, 012073 (2017).